Appendix E
FCT Document Cover Sheet

Name/Title of Deliverable/Milestone: Metal Corrosion Mechanisms Milestone Report M4FT-14PN0804041 "Contribution to L2 Milestone: SNL Overall Control Account"

Work Package Title and Number: FT-14PN080404 – Waste Form Degradation Modeling - PNNL

Work Package WBS Number: 1.02.08.04 Milestone Number: M4FT-14PN0804041

Responsible Work Package Manager

Frances Smith (Name/Signature) 22-Jul-2014 (Date Submitted)

Quality Rigor Level for Deliverable/Milestone	☒ QRL-3	☐ QRL-2	☐ QRL-1 ☐ Nuclear Data	☐ N/A*

This deliverable was prepared in accordance with Pacific Northwest National Laboratory
(Participant/National Laboratory Name)

QA program which meets the requirements of
☒ DOE Order 414.1 ☐ NQA-1-2000 ☐ Other: _____

This Deliverable was subjected to:
☒ Technical Review ☐ Peer Review

Technical Review (TR)
Review Documentation Provided
☐ Signed TR Report, or
TR Report No.: _____
☐ Signed TR Concurrence Sheet (attached), or
☐ Signature of TR Reviewer(s) below

Peer Review (PR)
Review Documentation Provided
☐ Signed PR Report, or
PR Report No.: _____
☐ Signed PR Concurrence Sheet (attached), or
☐ Signature of PR Reviewers below

Name and Signature of Reviewers

Bruce McNamara	15-Jul-14
(Name/Signature)	(Date)

*Note: In some cases there may be a milestone where an item is being fabricated, maintenance is being performed on a facility, or a document is being issued through a formal document control process where it specifically calls out a formal review of the document. In these cases, documentation (e.g., inspection report, maintenance request, work planning package documentation, or the documented review of the issued document through the document control process) of the completion of the activity along with the Document Cover Sheet is sufficient to demonstrate achieving the milestone. QRL for such milestones may also be marked N/A in the work package provided the work package clearly specifies the requirement to use the Document Cover Sheet and provide supporting documentation.

July 11, 2014

To: David Sassani (SNL)

From: Frances N. Smith

Cc: John Vienna (PNNL) Laura Buchanan (PNNL)

Approved by: _____

Name, Technical Reviewer Date

Approved by: _____

Name, Program Manager Date

Title: "Contribution to L2 Milestone: SNL overall Control Account" - Metal Corrosion Mechanisms

Milestone: M4FT-14PN0804041

"Contribution to L2 Milestone: SNL overall Control Account"

Metal Corrosion Mechanisms Milestone: M4FT-14PN0804041

Prepared for

U.S. Department of Energy

Used Fuel Disposition Campaign

Frances N. Smith

Pacific Northwest National Laboratory

July 11, 2014

FCRD-UFD-2014

Figures

Tables

Acronyms and Abbreviations

AFM	Anti-Ferromagnetic
AFM-P	Anti-Ferromagnetic Prime
AFM-DP	Anti-Ferromagnetic Double Prime
ANL	Argonne National Laboratory
DFT	Density Functional Theory
DOE	United States Department of Energy
EBS	Engineered Barrier System
FCRD	Fuel Cycle Research & Development
FM	Ferromagnetic
FR	Fractional Release
GOPT	Geometry optimized
LANL	Los Alamos National Laboratory
MWF	Metallic Waste Form
NE	Nuclear Energy
PNNL	Pacific Northwest National Laboratory
PIC	PNNL Institutional Computing
RN	Radionuclide
SNL	Sandia National Laboratory
SPE	Single-Point Energy
UFD	Used Fuel Disposition
UHF	Unrestricted Hartree Fock
UNLV	University of Nevada Las Vegas

Summary

This report describes the work performed to meet milestone M4FT-14PN0804041, "*Contribution to L2 Milestone: SNL Overall Control Account*," for the FT-14PN0804042, "*Metal Corrosion Mechanisms*" project under FT-14PN080404, "*Waste Form Degradation Modeling*" at Pacific Northwest National Laboratory (PNNL). This work is part of a multi-institutional effort involving experiment and theory to understand the fate of technetium (Tc) during the corrosion of iron-based metallic waste forms. This past year, significant efforts were made to connect Metallic Waste Form (MWF) research outcomes to Used Fuel Disposition (UFD) campaign needs to help achieve common research objectives. In this report, an update is provided on the status of atomic-scale modeling of Tc incorporation in to the iron oxy-hydroxide, goethite (α-FeOOH), a common corrosion product of steel and the most commonly occurring iron oxy-hydroxide in nature, as well as a potential waste form itself. This project is divided into three main parts: 1) determining Tc incorporation mechanisms into the bulk goethite structure, 2) determining Tc affinity for bulk versus surface environments, and 3) determining Tc stability in (near-) surface goethite environments in the presence of adsorbates. Here, an update will be provided on the first phase, bulk incorporation methods.

Metal Corrosion Mechanisms Milestone Report M4FT-14PN0804041 "Contribution to L2 Milestone: SNL Overall Control Account"

Frances N. Smith

Pacific Northwest National Laboratory, Richland, WA

Contents

Executive Summary

Introduction

During the reprocessing of commercial nuclear fuels or the vitrification of high-level defense waste, technetium (Tc) is an element of concern due to its volatility and tendency to partition among different waste streams (Darab and Smith, 1996; Um et al., 2011; McCloy et al., 2012). As such, separate waste forms are often considered for stabilizing Tc, such as borosilicate glasses (Darab and Smith, 1996; McCloy et al., 2012), metallic iron-technetium alloys (Taylor, 2011a,b), technetium sulfides, as well as iron oxides and iron oxy-hydroxides (Um et al., 2011 and references therein). The solution of capturing Tc in metallic waste forms (MWFs; e.g., Fe-Tc alloys) as part of the separations and/or vitrification process is of interest because Tc-stainless steel alloys offer high waste loading and promising corrosion resistance (Taylor, 2011); however, it is still important to consider the long-term corrosion behavior of these materials since it affects our understanding of the Tc source term in a repository environment. Technetium is an element of concern during the long-term storage of nuclear materials because of its long half-life (2.1×10^5 years), high-mobility in the environment as the oxidized pertechnetate anion ($Tc(VII)O_4^-$), and radiotoxicity as a beta emitter (Lieser and Bauscher, 1987; Meyer et al., 1991). While experiments can answer the question of "*Does Tc get incorporated into steel corrosion products?*" atomic-scale modeling provides a method for answering, "*How is Tc incorporated into steel corrosion products?*" These questions are important to address since they have implications for the capacity of iron oxides and iron oxy-hydroxides to retain Tc and other radionuclides in a long-term storage environment.

Here, atomic-scale modeling methods are used to investigate the incorporation of Tc into the iron oxy-hydroxide phase, goethite (α-FeOOH). Goethite was chosen for many reasons: 1) it is the most common iron oxy-hydroxide in nature (Alvarez et al., 2008); 2) it is a common steel corrosion product (Oh et al., 1999; Dodge et al., 2002); and 3) experimental results demonstrate that goethite can incorporate Tc(IV) into its structure, leading to the proposal of goethite as a waste form for Tc, as well (Um et al., 2011, 2012). With respect to the last point, uncertainty still remains as to the method of Tc(IV) incorporation into the goethite which has implications for Tc-fate during the corrosion of MWFs, as well as corrosion products as hosts for

radionuclides in a repository environment. As such, three main research objectives are being addressed in this study using atomic-scale (quantum-mechanical) modeling techniques to determine: 1) the most favorable Tc incorporation mechanisms into the bulk goethite structure, 2) Tc affinity for bulk versus surface environments of goethite, and 3) determining Tc stability in (near-) surface goethite environments in the presence of adsorbates, such as water (H_2O), oxygen (O_2), hydrogen (H_2), and hydrogen peroxide (H_2O_2). These species are under consideration because they contribute to our understanding of the long-term behavior of waste-form materials in storage environments, including scenarios involving radiolysis. Here, an update will be provided on the first objective, bulk incorporation methods.

Methods

Quantum-Mechanical Calculations

Charge-localized, quantum-mechanical methods are being used to explore possible Tc incorporation scenarios in bulk goethite. Specifically, the modeling software CRYSTAL09 (Dovesi et al., 2005) is being used to calculate single-point energies and optimized geometries for bulk goethite models. From these models, charge-balanced, coupled substitution mechanisms will be evaluated to calculate Tc incorporation energies. The unrestricted Hartree Fock (UHF) level of theory, that allows for unpaired electronic spin, is being used based on previously successful modeling efforts involving the Tc-hematite system where discrete Fe(II)/Fe(III) and Tc(IV)/Tc(VII) charge distinctions were maintained during structure and energy optimizations (Skomurski et al., 2010a, and references therein). While combined HF-Density Functional Theory (DFT) methods may ultimately be used to more thoroughly account for the exchange and correlation contributions to the ground-state energy of the system (i.e., UHF methods account for exchange but not correlation energy contributions), UHF methods have been demonstrated to successfully capture localized electron behavior in iron oxides (Rosso et al., 2003; Iordanova et al., 2005). These hybrid HF-DFT calculations can take place once initial UHF calculations are completed, using pre-optimized structures as a starting point to conserve computational time.

The first step in any modeling study is to determine the calculation parameters that are most appropriate for the system of interest, specifically basis-set testing, run parameter optimization, and capturing magnetic or electronic structure of the specific material. Basis sets being used for

iron and technetium in this study were demonstrated to effectively capture discrete Fe(II) and Fe(III) behavior in previous studies on iron charge distribution in magnetite ($Fe(II)Fe(III)_2O_4$; Skomurski et al., 2010b.), and Tc (IV) versus Tc(VII) behavior in a study on Tc incorporation into hematite ($Fe(III)_2O_3$; Skomurski et al., 2010a and references therein). Run parameter testing led to a k-point density selection of 63 electronic sampling points in crystallographic space; higher k-point densities lead to a one-order of magnitude improvement in energy convergence relative to the previous k-point density selection (e.g., 2×10^{-3} eV versus 2×10^{-4} eV energy change for 63 versus 36 k-points and 112 versus 63 k-points, respectively; see **Table 1**). While a higher k-point density could be considered for final calculations, 63 k-points are sufficient for testing a wide variety of goethite models.

Table 1. Total energy versus k-point density in a single, ferromagnetic (FM) goethite unit cell.

Shrinking Factor	# k-points	Single-Point Energy (Ha)	Energy Diff. (n-(n-1)) (Ha)	Energy Diff. (n-(n-1)) (eV)
1 1	1	-772.70401	NA	NA
2 2	8	-214.09426	558.60975	15200.32989
3 3	14	-214.11287	-0.01861	-0.50652
4 4	36	-214.11397	-0.00110	-0.02987
5 5	63	-214.11405	-0.00008	-0.00227
6 6	112	-214.11406	-0.00001	-0.00017

*Here, "n" refers to the current case, and "n-1" to the previous case.

In **Table 1**, energies in column four are reported in Hartrees and converted to electron volts (eV) in column five (1 Ha = 27.211 eV). In these calculations, the atomic positions, lattice parameters, and magnetic ordering of the iron atoms stayed the same while only the k-point density changed. Here, a ferromagnetic (FM) case was used where all iron atoms had the same direction of unpaired spins (e.g., all up or all down). A significant change in energy occurs when k-point density increases from 1 k-point in crystallographic space to 8 k-points; this result suggests that the single k-point was not robustly capturing the electronic structure of the goethite unit cell. Based on the minimal change in energy between 112 versus 63 k-points, the latter was chosen for all models to maximize computational resources while appropriately capturing the behavior of atoms in the goethite unit cell.

Regarding the magnetic structure of goethite, experimental studies suggest that it is antiferromagnetic at room temperature meaning it has no net-magnetic moment (Forsyth et al., 1968; Yang et al., 2006; Llavona et al., 2012). To achieve this, the four iron atoms in the unit cell must have equal and opposite, unpaired spin directions (e.g., 5 unpaired d-orbital electrons per each Fe^{3+}). Different spin structures can be assigned and maintained during energy or geometry optimization of the unit cell. Four different magnetic ordering schemes were tested and will be discussed in the Results section.

Incorporation Energy Calculations

The following schematic is used to describe the method for calculating incorporation energy (E_{inc}) using atomic-scale models (i.e., solid-phase energies for the pure and doped-bulk models and gas-phase energies for the elements being substituted, e.g., Tc(IV), Fe(II), and Fe(III)):

Figure 1. Schematic illustrating one possible charge-compensated substitution scheme where Tc(IV) and Fe(II) replace two lattice Fe(III) in bulk goethite. Blue rectangular prisms represent pure bulk goethite (left) and bulk goethite with substituted impurities (right). The right-hand side is the "Products" and the left-hand side is the "Reactants."

Here, the blue box on the left represents the pure (un-doped) iron oxide phase, and the Tc(IV)/Fe(II)-doped or "defect" iron oxide phase on the right. In this case, two Fe(III) cations are removed to accommodate a charge-balanced substitution of Tc(IV) and Fe(II) into the bulk. The E_{inc} is the sum of the optimized energy for the doped iron oxide case and excised Fe(III) cations on the right, minus the sum of the energy of the optimized pure iron oxide plus the Tc(IV) and Fe(II) cations on the left. A negative incorporation energy would indicate favorable incorporation of the Tc(IV)/Fe(II) pair, while a positive energy would indicate unfavorable incorporation of the impurities. The cations being added or removed are being treated as gas phase species by calculating the energy of an atom in a box (e.g., 10×10×10 $Å^3$) and accounting for its ionization energy. The pure and defect-phase bulk calculations are performed on infinite crystals (e.g., solids repeating infinitely in three-dimensions). Alternatively, solid-phase

references can be used for the impurity phases, such as $TcO_2 \cdot xH_2O$ for Tc(IV), following the method described by Shuller et al. (2013). Solvation energies can be applied impurity cations, as well, to simulate a more realistic, aqueous-based incorporation scenario. Previous studies suggest that this additional calculation may affect the magnitude of the incorporation energies, but not necessarily the trends, based on energy calculations of uranyl carbonate molecules treated as gas-phase, coordinated by water molecules, and subjected to a polarizable continuum model to simulate water (Schlosser et al., 2010). Such calculations could be considered when finalizing energies for Tc-incorporation models being develop here. Different Tc substitution schemes will be discussed in the Results section.

Single Unit Cell and Supercell Models

A single goethite unit cell is orthorhombic with *Pbnm* space-group symmetry, and contains 16 atoms (see **Figure 2**). All structures in this paper have been built according to the lattice and atomic positions described in Yang et al. (2006) for a single crystal of goethite, where a = 4.5979 Å, b = 9.9510 Å, and c = 3.0178 Å; α, β and γ are all 90°. In goethite, each iron atom is octahedrally coordinated by 3 oxygen atoms and 3 hydroxyl groups. Two Fe atoms in the center of the unit cell are edge-sharing, and each of those Fe atoms shares a corner with an additional Fe atom at the top right and bottom left corners of the unit cell (see **Figure 2**). When extended in three dimensions, all Fe atoms share edges with Fe atoms in neighboring unit cells, forming chains parallel to the *c*-axis (i.e., into the paper). Another way to describe the unit cell is that half of the octahedral sites created by the oxygen sub-lattice are occupied by Fe atoms.

The motivation for using supercells to study Tc incorporation into goethite is to achieve experimentally-relevant Tc incorporation levels. For instance, by substituting a single Fe atom in a single unit cell with Tc, an impurity loading of 25 atomic % would result. For prior studies of Tc incorporation into hematite, 1-3 atomic % impurity loading was of interest based on experimental data (Skomurski et al., 2010 and references therein). While exact limits of Tc incorporation into goethite are not currently well established, there is interest in using models with more iron atoms such that a broad range of incorporation percentages can be explored. However, a trade-off exists between the number of atoms in a system and computational time. In **Table 2**, the number of atoms per $n \times n \times n$ supercell is presented, where n is the number of single unit cells per side of the supercell. A 3×3×3 unit cell containing 432 atoms was settled upon such

that a substitution of one Tc atom for one Fe atom is approximately 1 atomic % impurity in the system (highlighted in bold in **Table 2**).

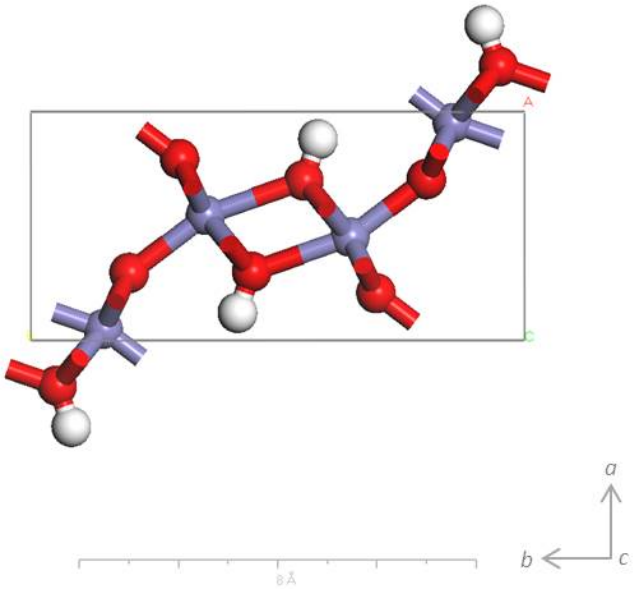

Figure 2. A single unit cell of goethite looking down the *c* axis. Purple spheres are iron, red spheres are oxygen, and white spheres are hydrogen. A scale bar is included for reference.

Table 2. Number and type of each atom in a goethite supercell when increasing dimensions by $n \times n \times n$ unit cells.

# Unit Cells / Side	# Iron Atoms	# Hydrogen Atoms	# Oxygen Atoms	# Total Atoms
1×1×1	4	4	8	16
2×2×2	32	32	64	128
3×3×3	**108**	**108**	**216**	**432**
4×4×4	256	256	512	1024
5×5×5	500	500	1000	2000
6×6×6	864	864	1728	3456
7×7×7	1372	1372	2744	5488
8×8×8	2048	2048	4096	8192
9×9×9	2916	2916	5832	11664
10×10×10	4000	4000	8000	16000

Results

Magnetic Structure Calculations

As mentioned earlier, goethite exhibits antiferromagnetic behavior at room temperature (Yang et al., 2006; Forsyth et al., 1968; Llavona et al., 2012). Because each Fe(III) in the single goethite unit cell has five unpaired electrons in the same spin up or spin down orientation, each Fe(III) carries a net spin of 5. In order to cancel out the net spin of the unit cell, half the iron atoms must have opposite spins compared to the other half. In **Figure 3**, four different magnetic structures are illustrated: (a) ferromagnetic (FM) where all atoms have the same spin direction; (b) anti-ferromagnetic (AFM) where edge-sharing Fe(III) have opposite spin directions to each other and the corner sharing Fe(III) atoms; (c) anti-ferromagnetic-prime (AFM-P) where edge-sharing Fe(III) have the same spin and opposite spin from the corner sharing Fe^{3+}; and (d) anti-ferromagnetic double-prime (AFM-DP) where edge sharing Fe(III) have opposite spin, but the same spin as neighboring, corner sharing Fe(III). The FM case has a net spin of 20 per unit cell; all other AFM cases have a net spin of 0.

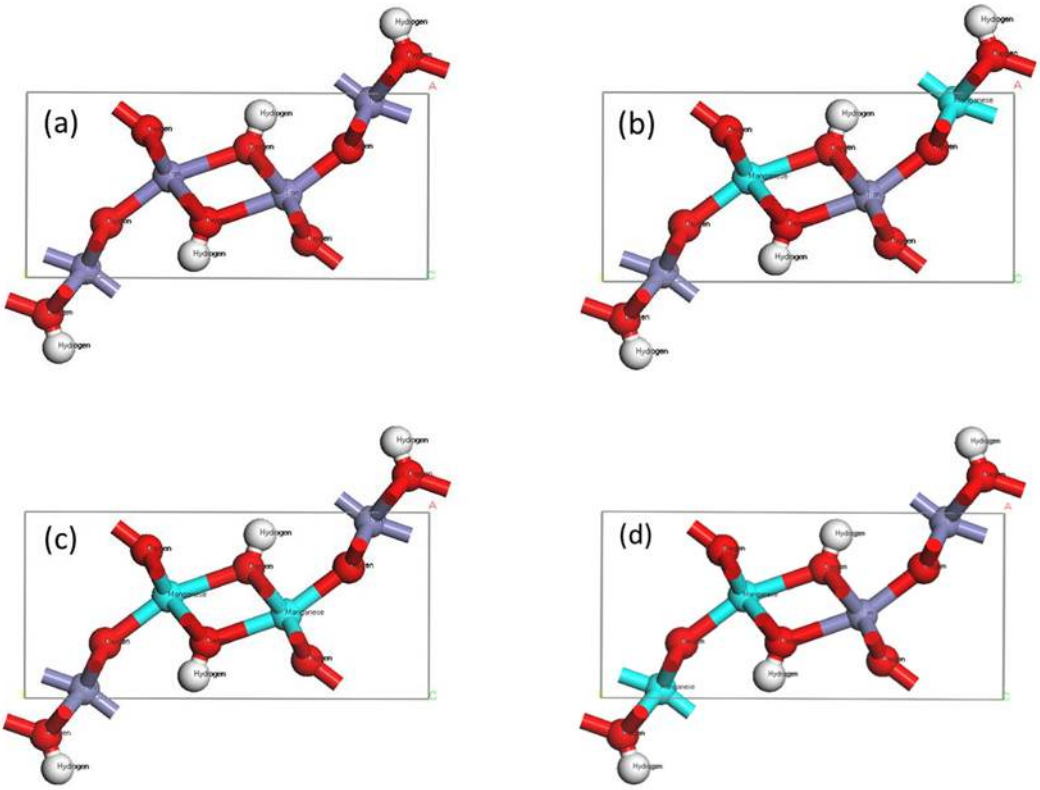

Figure 3. Four different magnetic structures for goethite represented by a single unit cell: a) ferromagnetic (all Fe(III) are spin up); b) anti-ferromagnetic (edge sharing Fe(III) octahedra have opposite spins); c) anti-ferromagnetic prime (edge-sharing Fe(III) octahedra have the same spin); and d) anti-ferromagnetic double-prime (edge-sharing Fe(III) octahedra have opposite spins; corner sharing Fe(III) octahedra have the same spin). Purple spheres are Fe(III) (spin up), aqua spheres are Fe(III) (spin down), red spheres are O, and white spheres are H.

In order to test for the lowest-energy magnetic structure, single point energy (SPE) calculations were performed on each of the unit cells shown above. Subsequently, geometry optimizations (GOPT), where only the atoms (not the lattice parameters) were allowed to move, were performed on the same models for comparison. Results are shown in **Table 3.**

Table 3. Single-point energy versus geometry optimized calculations for single goethite unit cells with different magnetic ordering on the iron sub-lattice.

Filename	**# k points**	**Total Energy (Ha)**	**Fe spins (×2)**	**Energy Difference* (Ha)**	**Energy Difference* (eV)**
FM Case (SPE)	63	-214.11405	± 4.798	---	---
FM Case (GOPT)	63	-214.16487	± 4.808	-0.05082	-1.38284
AFM Case (SPE)	63	-214.11701	± 4.782	---	---
AFM Case (GOPT)	63	-214.16698	± 4.795	-0.04997	-1.35980
AFM-P Case (SPE)	63	-214.11724	± 4.784	---	----
AFM-P Case (GOPT)	63	-214.16724	± 4.797	-0.05001	-1.36074
AFM-DP Case (SPE)	63	-214.11375	± 4.796	---	---
AFM-DP Case (GOPT)	63	-214.16451	± 4.806	-0.05076	-1.38134

* Energy difference refers to cases with atomic positions optimized (EOPT) minus single-point energy cases (SPE), those without atomic-positions optimization.

Looking at "Total Energy" values for all cases tested, the GOPT values are approximately 0.05 Ha, or 1.36 eV lower in energy than the single-point energy calculations. This result is expected since by atoms will move to find their lowest-energy position along calculated energy gradients with respect to the assigned atomic basis sets. When comparing SPE-optimized

models in column 3, the AFM-P and AFM cases are nearly equivalent for the lowest energy, followed by the FM case, and the AFM-DP case with the least favorable optimized energy of all. For the two lowest-energy cases, the energy difference is approximately 0.0002 Ha, or 0.0054 eV. For the two highest-energy cases, the energy difference is of similar magnitude; however, the low cases versus the high cases are about 0.05 eV different in energy. The same trend is apparent when analyzing the GOPT results, where AFM-P and AFM cases are nearly equivalent with the lowest energy values, followed by the FM case, and the AFM-DP case with the highest optimized energy values. Values are similar, too with the two lowest cases differing by only 0.0003 Ha, or 0.0073 eV. Differences between the lowest-energy magnetic structures (AFM-P) and the highest-energy cases (AFM-DP) are an order of magnitude greater in energy (e.g., 0.095 and 0.074 eV) for both SPE and GOPT calculations, respectively.

When comparing these results to computational studies on fully-geometry optimized goethite models found in the literature, the AFM and AFM-P magnetic ordering cases have the lowest reported energies, with the AFM structure being slightly more favorable than the AFM-P structure, according to Guo and Barnard (2012). Least favorable is the AFM-DP case, followed by a ferromagnetic case. In a modeling study by Fuente et al. (2013), similar results were obtained with the AFM case being the lowest in energy of the three different AFM cases tested. This difference in lowest-energy trends may exist because lattice parameters were not yet allowed to relax fully in this study, for which further testing will be performed. Experimental Mössbauer spectroscopy studies also suggest that the AFM structure is also observed at room temperature (Forsythe et al., 1968); however, recent papers outline the complexity in determining the magnetic structure in goethite due to some magnetic orderings exhibiting similar energies to one another (Pankhurst et al., 2012). Moving forward, the two lowest energy magnetic structures determined here, AFM and AFM-P, will be used to generate super cells and Tc-incorporation models, although only AFM models will be illustrated in the following section.

Bulk Incorporation Models

Goethite is known to host many metal and metalloid impurities in nature such as aluminum manganese, chromium and nickel (Alvarez et al., 2008). In recent studies by Um et al. (2011, 2012), where Tc-bearing goethite was precipitated in the presence of Fe(II) and the pertechnetate anion, TcO_4^-, strong spectroscopic evidence points towards the incorporation of Tc into goethite

as Tc(IV) rather than Tc(VII), or the pertechnetate anion. Based on the similarity in atomic radii between Tc(IV) and Fe(III), substitution into the octahedral Fe site is likely feasible. This type of mechanism is supported by previous modeling efforts where Tc(IV) was found to favorably substitute for Fe(III) in the hematite structure, along with the transformation of two Fe(III) to Fe(II) for charge balance (Skomurski et al., 2010a). Although goethite and hematite have different chemistries and structural arrangements of atoms, the Fe(III) coordination environment between them is similar and they are part of a temperature-based transformational series favoring hematite over goethite as temperature increases (Gualtieri and Venturelli, 1999). As such, it is possible that similar Tc(IV) substitution mechanisms could be favored in both (see **Figure 4a**).

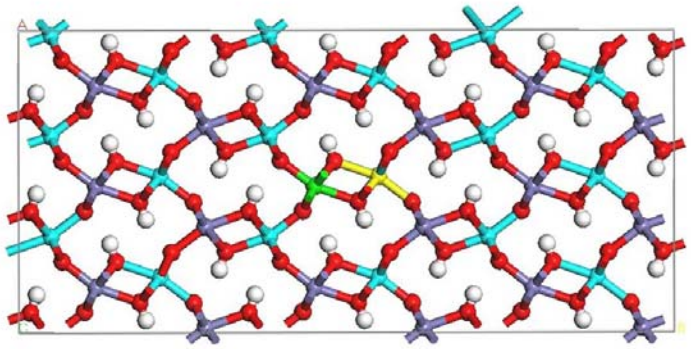

(a)

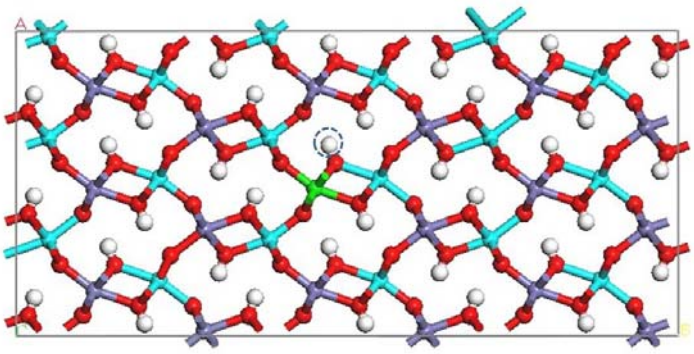

(b)

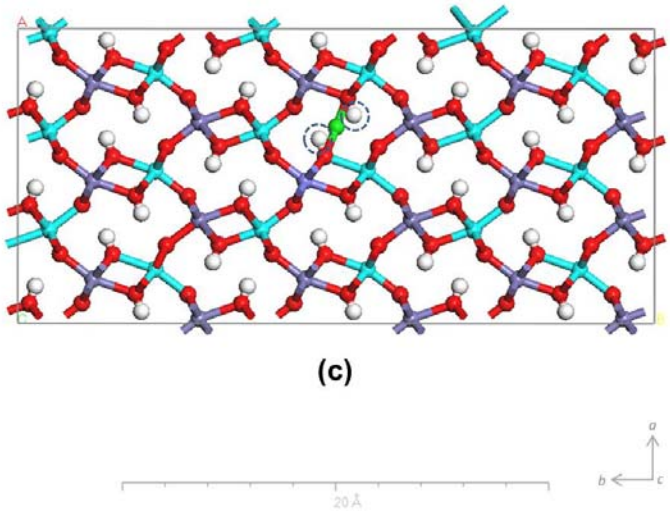

Figure 4. Goethite supercells (3×3×3) representing the anti-ferromagnetic (AFM) spin structure illustrating three different Tc(IV) substitution schemes: a) coupled Tc(IV) (green) / Fe(II) (yellow) substitution for two lattice Fe(III); b) Tc(IV) substitution of one lattice Fe(III) and removal of one H^+ for charge balance; and c) interstitial Tc(IV) addition to the supercell and removal of four nearest-neighbor H^+ for charge balance. A 20 Å scale-bar is included for reference. Purple spheres are Fe(III) (spin up), aqua spheres are Fe(III) (spin down), red spheres are O^{2-}, and white spheres are H^+; additionally, green spheres are Tc(IV) spin up and yellow spheres are Fe(II) spin down.

In contrast to hematite, where excess Fe(II) is observed in the Fe_2O_3 structure upon incorporation of M^{4+} impurities, such as titanium, where *M* stands for metals (Droubay et al., 2007), a study by Berry et al. (2000) suggests that no excess Fe(II) is observed in the goethite upon substitution of Sn(IV) for Fe(III) when X-ray photoelectron spectroscopy (XPS) was used to probe samples. Instead, a number of direct or interstitial Sn(IV) substitutions for Fe(III) were tested using empirical potential modeling methods to account for experimental observations. In that case, a coupled Fe(III) + vacancy substitution had the lowest energy, followed by coupled Fe(III) + OH- vacancies, Fe(III) + O2- vacancies, with an interstitial Sn(IV) having the highest, or least favorable, incorporation energy (Berry et al., 2000). Out of those models described in that paper, two mechanisms are being tested here, one where Tc(IV) replaces a lattice Fe(III) directly, and the nearest H^+ is removed for remaining charge balance (**Figure 5b**), and another case where interstitial Tc^{4+} occupies and empty Fe-octahedral site, charge compensated by

removing four nearest-neighbor H^+ to maintain charge neutrality (**Figure 5c**). These three models are being used as a starting point for SPE and GOPT energy calculations that will ultimately be coupled with incorporation energy calculations, as outlined in **Figure 1**, to determine which Tc(IV) incorporation mechanisms are most favorable in goethite. Additional models, as described for UO_2^{2+} substitution into iron oxides by Kerisit et al. (2011) will also be used as a guide for exploring the parameter space for Tc(IV) incorporation into goethite.

Once the most energetically favorable Tc incorporation scheme is identified, additional goethite super cells will be generated into which increasing amounts of Tc can be added in the same fashion. In this way, the effect of Tc loading on E_{inc} can be evaluated to determine if there is an incorporation limit for Tc in the goethite structure, or at least if a limit is approaching. Ultimately, surface slabs will be generated using the most stable incorporation mechanism to investigate the effect of free surfaces and adsorbates on Tc stability in iron oxide corrosion products of metallic Fe-Tc waste forms.

Discussion

Connections to Metallic Waste Form Research Objectives

The Tc incorporation into goethite modelling effort described here is part of a larger body of modeling and experimental studies being performed on Tc-bearing MWFs at Los Alamos National Laboratory (LANL) and the University of Nevada Las Vegas (UNLV. Specifically at LANL, MWF-oxide interfaces are being studied using electrochemical and surface-characterization methods, in addition to fundamental corrosion studies being performed on MWF using atomic-scale modeling methods, building on previous work in this area. At UNLV, atomic-scale modeling efforts are focused on understanding Tc-incorporation and metal diffusion in a series of increasingly oxidized iron oxides (e.g., FeO to Fe_3O_4 to Fe_2O_3, etc.) to understand incorporation mechanisms and Tc stability as a function of oxidation and the presence of other transition metals. The differences between modeling efforts at PNNL and UNLV is the use of iron oxy-hydroxide phases versus iron oxides, respectively, and the ultimate trajectory of focusing on Tc stability at goethite-environmental interfaces at PNNL versus the bulk behavior or Tc in different iron oxides at UNLV.

During the current fiscal year (FY14), discussion increased among individuals at different institutions working on research under the umbrella the "*Metal Corrosion Mechanisms*" project (FT-14PN0804042) to ensure that common and complementary research goals were being met at PNNL, LANL, and UNLV. These efforts are highlighted in **Figure 5**. Along those lines, it was important to ensure that experimental and theoretical research results could also be explained in context of a larger-scale, fractional release (FR) model (see **Figure 5**) that could be of direct use to understanding radionuclide behavior in a generic repository environment. Argonne National Laboratory (ANL) spear-headed discussions to understand where contributions from all areas of "*Waste Form Degradation Modeling*" research fit into this equation. Increased awareness of others' research and having a common, high-level framework to work in has helped coordinate research efforts and maintain focus on how these results can be applied to Department of Energy, Nuclear Energy, Fuel Cycle and Research Development (DOE-NE-FCRD) needs. These connections were facilitated by monthly telecom meetings led by Sandia National Laboratory (SNL) to help integrate MWF research efforts into Used Fuel Disposition (UFD) research goals, as well.

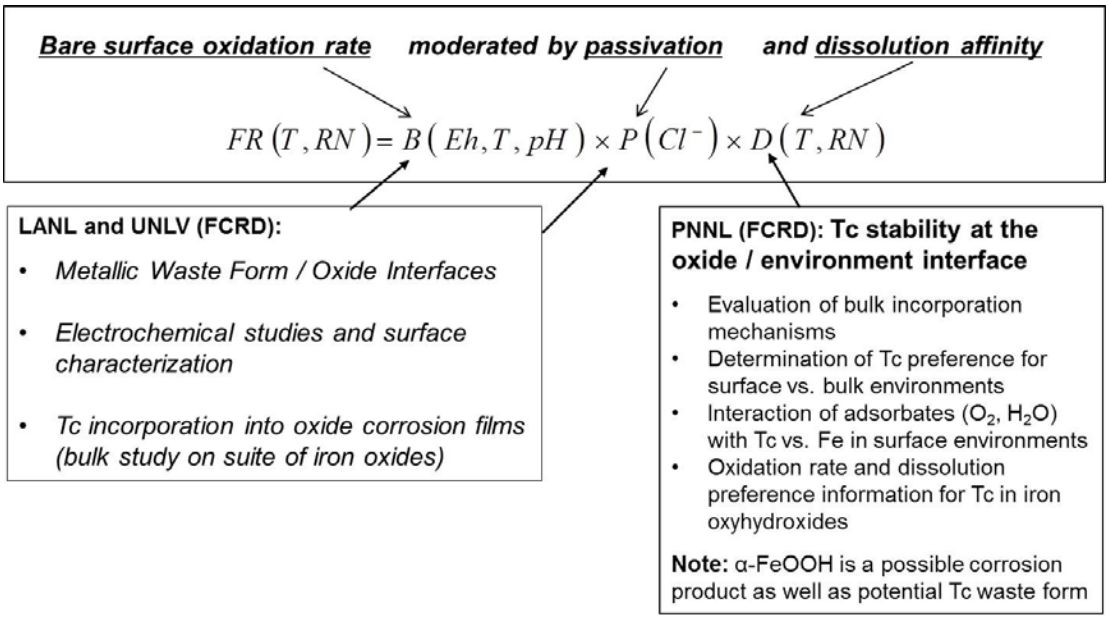

Figure 5. Schematic illustrating how "*Metal Corrosion Mechanisms"* research at PNNL, LANL, and UNLV contributes to a conceptual model describing fractional release (FR) of radionuclides from MWF (equation provided by William (Bill) Ebert, Argonne National Laboratory; research details compiled by F. Smith, PNNL; X. Liu, LANL; and E. Kim, UNLV).

In brief, the FR equation above was used as a framework to understand where research results from "*Metal Corrosion Mechanisms*" projects fits into the components of the equation, where *B* is a bare surface oxidation rate as a function of Eh, T, and pH; *P* is a passivation term that can be affected different ion concentrations or species present in solution; and *D* is a dissolution affinity term that depends on temperature and radionuclide species. As seen in the bottom right corner of **Figure 5**, the study of Tc incorporation into iron oxy-hydroxides at PNNL feeds the dissolution affinity term most directly by, 1) understanding how, and how much, Tc is incorporated into the goethite structure; 2) by evaluating whether Tc prefers a surface versus bulk environment in goethite which affects its availability for release, and 3) understanding how strongly Tc interacts with adsorbates when in the goethite structure. Ultimately, reaction rates for Tc oxidation will be calculated when the third phase of this research project is reached. Experimental and theoretical research at LANL and UNLV (bottom left corner of **Figure 5**) contribute more directly to the bare surface oxidation rate term, as well as the passivation rate term. Technetium incorporation into iron oxides being performed at UNLV can also feed into the dissolution affinity term by understanding bulk incorporation mechanisms and in that study, diffusion behavior of metals in MWFs and metal oxides. By having this framework, researchers at different institutions can ensure that results are complementary and moving towards a common goal.

Connections to Used Fuel Disposition Research Objectives

While the Tc incorporation into iron oxy-hydroxides research described here stems from MWF origins, it has broad application to UFD research objects, largely due to the potential for significant amounts of iron in a repository environment to interact with stored radionuclides. Using **Figure 6**, various source terms in an Engineered Barrier System (EBS) will be highlighted to illustrate where Tc (or radionuclide) interaction with iron oxides will play an important role in predicting waste form performance in a long-term storage scenario. First and foremost is the waste form itself. For a MWF, Tc would be a large component of a metal-alloy waste. As such, the degradation of the waste form (**Figure 6**, bottom left corner) needs to be understood as some "*Metal Corrosion Mechanisms*" research efforts are investigating (LANL and UNLV). For this study in particular, the "Radionuclide Mobilization and Transport" source term (**Figure 6**, top right corner) is being addressed most directly by asking the question of, "*How is Tc incorporated into iron-oxyhydroxide corrosion products of MWF?*", and ultimately, "*How stable is Tc in iron oxy-hydroxide corrosion products in the presence of adsorbates?*" By understanding the ability of iron oxides and iron oxy-hydroxides to incorporate Tc and at what limits,

the potential for these phases to serve as sinks for mobilized radionuclides is increased. These phenomena ultimately have implications for the "Source Term" box at the top of **Figure 6**, where RN interaction with iron oxides has influences on RN mobilization behavior.

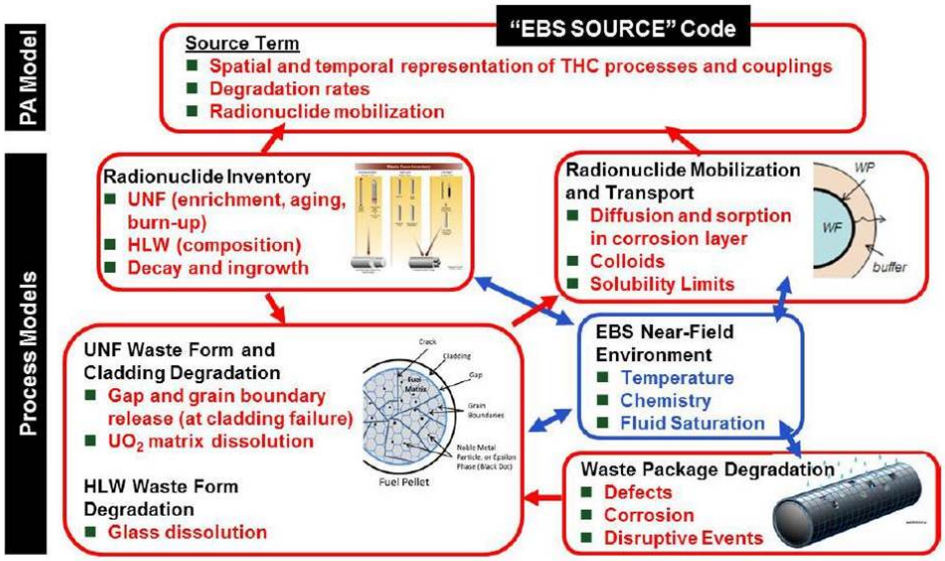

Figure 6. Schematic illustrating different processes that contribute to an overall understanding of radionuclide source terms for a generic disposal system. The individual "Process Models," including inventory, waste form, and waste package degradation processes, ultimately feed into the radionuclide source term as part of a "Probabilistic Assessment" (PA) Model. Figure borrowed from Freeze et al. (2013) FCRD-UFD-2014-000062 (Figure 2-11).

From a UFD stand point alone, Tc is an element of concern due to its long half-life, high mobility in the environment as the oxidized pertechnetate anion (TcO_4^-), and its radiotoxicity (Lieser and Bauscher, 1987; Meyer et al., 1991). In irradiated fuel, Tc makes up approximately 6% of total fission product content and is found in the epsilon metal phase that precipitates out at grain boundaries or even within the grain (Kleykamp, 1985; Cui et al., 2004; Bruno and Ewing, 2006; Um et al., 2011). As such, if waste packages are compromised, and ultimately the fuel matrix, the likelihood of Tc interacting with environmental variables increases. Assuming that iron-bearing waste packages are used, then the "Waste Package Degradation" box (**Figure 6**, bottom right-hand corner) becomes increasingly significant since iron corrosion products (including goethite), will affect the "Radionuclide Mobilization and Transport" box as Tc could be incorporated into those phases. This process ultimately affecting radionuclide mobilization in

the "Source Term" box. Finally, waste package degradation may have significant effects on local Eh and pH conditions, as studies have shown that hydrogen gas could be generated due to corrosion and help maintain reducing conditions (Carbol et al., 2009); or, corrosion products may have a "self-sealing" effect on waste packages and help maintain the integrity of the fuel as a waste form by protecting it from further interaction with environmental variables (Ferriss et al., 2009). As such, radionuclide interaction with iron corrosion products will play a significant role in predicting the long-term behavior of used fuel or metallic waste forms in a repository environment.

Acknowledgements

This research was performed using PNNL Institutional Computing (PIC) at Pacific Northwest National Laboratory. The author wishes to thank D. Sassani, W. Ebert, X. Liu, E. Kim, and the entire UFD working group for useful discussions on research directions and coordination.

References

Alvarez, M., Sileo, E.E., and Rueda, E.H. (2008) Structure and reactivity of synthetic Co-substituted goethites. *American Mineralogist*, 93, 584-590.

Berry, F.J., Helgason, Ö., Bohórquez, A., Marco, J.F., McManus, J., Moore, E.A., Mørup, S., and Wynn, P.G. (2000) Preparation and characterization of tin-doped α-FeOOH (goethite). *Journal of Materials Chemistry*, 10, 1643-1648.

Bruno, J. and Ewing, R.C. (2006) Spent Nuclear Fuel. *Elements*, 2(6), 343-349.

Carbol, P., Fors, P., Gouder, T., and Spahiu, K. (2009) Hydrogen suppresses UO_2 corrosion. *Geochimica et Cosmochimica Acta*, 73, 4366-4375.

Cui, D., Low, J., Sjostedt, C.J., and Spahiu, K. (2004) On Mo-Ru-Tc-Pd-Rh-Te alloy particles extracted from spent fuel and their leaching behavior under Ar and H_2 atmospheres. *Radiochimica Acta*, 92, 551-555.

Darab, J.G. and Smith, P.A. (1996) Chemistry of technetium and rhenium species during low-level radioactive waste vitrification. Chemistry of Materials, 8, 1004-1021.

Dodge, C.J., Francis, A.J., Gillow, J.B., Halada, G.P., Eng, C., and Clayton, C.R. (2002) Association of uranium with iron oxides typically formed on corroding steel surfaces. *Environmental Science &Technology*, 36, 3504-3511.

Dovesi, R., Orlando, R., Civalleri, B., Roetti, C., Saunders, V. R. and Zicovich-Wilson, C. M. (2005) CRYSTAL: a computational tool for the ab initio study of the electronic properties of crystals. *Zeitschrift für Kristallographie*, 220, 571-573.

Droubay, T., Rosso, K.M., Heald, S.M., McCready, D.E., Wang, C.M., and Chambers, S.A. (2007) Structure, magnetism, and conductivity in epitaxial Ti-doped α-Fe_2O_3 hematite: Experiment and density functional theory calculations. *Physical Review B*, 75, 104412.

Ferriss, E.D.A., Helean, K.B., Bryan, C.R., Brady, P.V., and Ewing, R.C. (2009) UO_2 corrosion in an iron waste package. *Journal of Nuclear Materials*, 384, 130-139.

Forsyth, J.B., Hedley, I.G., and Johnson, C.E. (1968) The magnetic structure and hyperfine field of goethite (a-FeOOH). *Journal of Physics C (Proc. Phys. Soc.),* 2(1), 179-188.

Freeze, G., Gardner, W.P., Vaughn, P., Sevougian, S.D., Mariner, P., Mousseau, V., and Hammond, G (2013) Enhancements to Generic Disposal System Modeling Capabilities. FCRD-UFD-2014-000062, SAND2013-10532P, Sandia National Laboratories, Albuquerque, NM.

Fuente, S.A., Belelli, P.G., Castellani, N.J., and Avena, M. (2013) LDA+*U* and GGA+*U* studies of Al-rich and bulk goethite (α-FeOOH). *Materials Chemistry and Physics*, 137, 1012-1020.

Gualtieri, A.F. and Venturelli, P. (1999) In situ study of the goethite-hematite phase transformation by real time synchrotron powder diffraction. *American Mineralogist*, 84, 895-904.

Guo, H. and Barnard, A.S. (2011) Modeling the iron oxides and oxyhydroxides for the prediction of environmentally sensitive phase transformations. *Physical Review B*, 83, 094112.

Iordanova, N., Dupuis, M., and Rosso, K.M. (2005) Charge transport in metal oxides: a theoretical study of hematite α-Fe_2O_3. *Journal of Chemical Physics*, 122, 144305.

Kerisit, S., Felmy, A.R., and Ilton, E.S. (2011) Atomistic simulations of uranium incorporation into iron (hydr)oxides. *Environmental Science & Technology*, 45, 2770-2776.

Kleykamp, H. (1985) The chemical state of the fission products in oxide fuels. *Journal of Nuclear Materials*, 131, 221-246.

Lieser, K.H. and Bauscher, C. (1987) Technetium in the hydrosphere and in the geosphere I. Chemistry of technetium and iron in natural waters and influence of the redox potential on the sorption of technetium. *Radiochimica Acta*, 42, 205-213.

Llavona, Á., Prados, A., Velasco, V., Crespo, P., Sánchez, M.C., and Pérez, L. (2013) Electrochemical synthesis and magnetic properties of goethite single crystal nanowires. *CrystEngComm*, 15, 4905-4909.

McCloy, J.S., Riley, B.J., Goel, A., Liezers, M., Schweiger, M.J., Rodriguez, C.P., Hrma, P., and Kim, D.-S. (2012) Rhenium solubility in borosilicate nuclear waste glass: Implications for the processing and immobilization of technetium-99. Environmental Science & Technology, 46, 12616-12622.

Meyer, R.E., Arnold, W.D., Case, F.I., and O'Kelley, G.D. (1991) Solubilities of Tc(IV) oxides. *Radiochimica Acta*, 55(1), 11-18.

Oh, S.J., Cook, D.C., and Townsend, H.E. (1999) Atmospheric corrosion of different steels in marine, rural and industrial environments. *Corrosion Science*, 41, 1687-1702.

Pankhurst, Q.A., Barquín, L.F., Lord, J.S., Amato, A., and Zimmermann, U. (2012) Intrinsic magnetic relaxation in goethite. *Physical Review B*, 85, 174437.

Rosso, K.M., Smith, D.M>, and Dupuis, M. (2003) An ab initio model of electron transport in hematite (α-Fe2O3) basal planes. *Journal of Chemical Physics*, 118(14), 6455-6466.

Schlosser, F., Moskaleva, L.V., Kremleva, A., Kruger, S., and Rosch, N. (2010) Comparative density functional study of the complexes $[UO_2(CO_3)_3]^{4-}$ and $[(UO_2)_3(CO_3)_6]^{6-}$ in aqueous solution. *Dalton Transactions*, 39, 5705-5712.

Shuller, L.C., Ewing, R.C., and Becker, U. (2013) Np-incorporation into uranyl phases: A quantum-mechanical evaluation. *Journal of Nuclear Materials*, 434, 440-450.

Skomurski, F.N., Rosso, K.M., Krupka, K.M., and McGrail, B.P. (2010a) Technetium incorporation into hematite (α-Fe_2O_3). *Environmental Science & Technology*, 44, 5855-5861.

Skomurski, F.N., Kerisit, S., and Rosso, K.M. (2010b) Structure, charge distribution, and electron hopping dynamics in magnetite (Fe_3O_4) (100) surfaces from first principles. *Geochimica et Cosmochimica Acta*, 74, 4234-4248.

Taylor, C.D. (2011a) Cohesive relations for surface atoms in the iron-technetium binary system. *Journal of Metallurgy*, 2011, Article ID 954170, 1-8.

Taylor, C.D. (2011b) Surface segregation and adsorption effects of iron-technetium alloys from first-principles. *Journal of Nuclear Materials*, 408, 183-187.

Um, W., Chang, H.-S., Icenhower, J.P., Lukens, W.W., Serne, R.J., Qafoku, N.P., Westick, Jr., J.H., Buck, E.C., and Smith, S.C. (2011) Immobilization of 99-Technetium(VII) by Fe(II)-goethite and limited reoxidation. *Environmental Science & Technology*, 4904-4913.

Um, W., Chang, H., Icenhower, J.P., Lukens, W.W., Serne, R.J., Qafoku, N., Kukkadapu, R.K., and Westsik, J.H. Jr. (2012) Iron oxide waste form for stabilizing ^{99}Tc. *Journal of Nuclear Materials*, 429, 201-209.

Yang, H., Lu, R., Downs, R.T., and Costin, G. (2006) Goethite, α-FeO(OH), from single-crystal data. Acta Crystallographica, E62, i250-i252.